Radiation Physics and Chemistry 95 (2014) 185–187

Contents lists available at ScienceDirect

Radiation Physics and Chemistry

journal homepage: www.elsevier.com/locate/radphyschem

Monte Carlo simulation of liver cancer treatment with ^{166}Ho-loaded glass microspheres

Carla da Costa Guimarães [a,b], Maurício Moralles [c,*], José Roberto Martinelli [a]

[a] Centro de Ciência e Tecnologia de Materiais, Instituto de Pesquisas Energéticas e Nucleares IPEN/CNEN, Av. Prof. Lineu Prestes, 2242, CEP 05508-000, São Paulo-SP, Brazil
[b] Centro de Ciências Matemáticas Físicas e Tecnológicas, Pontifícia Universidade Católica de São Paulo, Av. Marquês de Paranaguá 111, CEP 01303-050, São Paulo-SP, Brazil
[c] Centro do Reator de Pesquisas, Instituto de Pesquisas Energéticas e Nucleares IPEN/CNEN, Av. Prof. Lineu Prestes, 2242, CEP 05508-000, São Paulo-SP, Brazil

HIGHLIGHTS

- Monte Carlo simulation of treatments with ^{166}Ho- and ^{90}Y-loaded microspheres.
- A voxelized anthropomorphic phantom and a simplified gamma camera were used.
- Volumetric dose map with 1.2 mm resolution was calculated.
- Image of the gamma camera was produced.
- Perspectives of treatment planning using Monte Carlo and GEANT4.

ARTICLE INFO

Article history:
Received 18 October 2012
Accepted 29 December 2012
Available online 7 January 2013

Keywords:
Brachytherapy
Microspheres
Monte Carlo
GEANT4
MASH phantom

ABSTRACT

Microspheres loaded with pure beta-emitter radioisotopes are used in the treatment of some types of liver cancer. The Instituto de Pesquisas Energéticas e Nucleares (IPEN) is developing ^{166}Ho-loaded glass microspheres as an alternative to the commercially available ^{90}Y microspheres. This work describes the implementation of a Monte Carlo code to simulate both the irradiation effects and the imaging of ^{166}Ho and ^{90}Y sources localized in different parts of the liver. Results obtained with the code and perspectives for the future are discussed.

© 2013 Elsevier Ltd. All rights reserved.

1. Introduction

The liver metastasis is one of the most common types of cancer that occur especially in patients with colorectal cancer. The position and extent of the patient's liver cancer define the choice of processing technique to be employed. Techniques commonly used in radiotherapy treatment of cancer were shown to be inefficient in treating this type of cancer because the liver parenchyma does not support high doses of radiation (Nijsen et al., 1999). Thus, brachytherapy with microspheres appears as a promising treatment for metastasis, since they are almost exclusively dependent on the arterial blood supply in comparison with normal liver, which receives most of its flow from the portal vein. Microspheres loaded with pure beta-emitting radioisotopes are administered via catheter into the patient through the hepatic artery being carried by blood flow and becoming entrapped in the capillaries of the tumor region. The beta particle energy is delivered mostly in the tumor so that healthy tissues are spared.

Nowadays there are two commercial microspheres loaded with ^{90}Y, made of glass and resin. Since ^{90}Y is a pure beta-emitter, the localization of the microspheres after injection is a difficult task, mainly based on SPECT images of the bremsstrahlung radiation produced by the beta particles. The Instituto de Pesquisas Energéticas e Nucleares (IPEN) is developing ^{166}Ho-loaded glass microspheres as an alternative to the ^{90}Y microspheres. The radioisotope ^{166}Ho is a promising alternative because, besides the beta emission with maximum energy of 1.85 MeV, it has a gamma ray of 81 keV with intensity of 6.7% that can be used for imaging with SPECT. The IPEN's microspheres have passed on tests of morphology (spherical

* Corresponding author. Tel.: +55 11 31339974.
E-mail address: moralles@ipen.br (M. Moralles).

0969-806X/$ - see front matter © 2013 Elsevier Ltd. All rights reserved.
http://dx.doi.org/10.1016/j.radphyschem.2012.12.050

shape and size), cytotoxicity and in vitro degradation (Barros Filho et al., 2012). In vivo tests with activated microspheres are planned as the next steps.

This work describes the implementation of a Monte Carlo code to simulate the irradiation effects and the imaging of radioactive sources distributed in the liver of an anthropomorphic phantom. The results obtained with ^{166}Ho and ^{90}Y sources localized in different parts of the liver are discussed.

2. Methodology

A Monte Carlo code that uses the GEANT4 toolkit (Agostinelli et al., 2003) was developed for the simulations of liver treatments with glass microspheres. The standard electromagnetic physics processes of GEANT4 were employed with a cut value for secondary particle generation of 100 μm for all particles. In GEANT4 the cut value for each type of particle is given as a mean free path, which is internally converted to an energy value for each different material (Agostinelli et al., 2003). The MASH anthropomorphic phantom in the form of cubic voxels of 1.2 mm (Cassola et al., 2010) was implemented in the code. The densities and tissues of the organs were the same as those used in the MAX phantom described by Kramer et al. (2006). The use of MASH produces an improvement in the description of anthropomorphic details when compared to MAX, which has cubic voxels of 3.6 mm.

An algorithm to simulate the liver tumor was developed to change liver voxels to tumor voxels as a fraction of the liver volume from 0 to 100%. The tumor grows radially from a starting voxel localized in one of seven possible positions: in the center or in one of the six extremities of the liver (superior, inferior, right, left, anterior and posterior). The modified voxel is simply labeled as a tumor voxel, but the voxel material is maintained the same as the liver material. The simulated treatment considers that all injected microspheres are uniformly distributed inside the tumor and, for simplicity, the glass matrix is not included. A previous work (Guimarães et al., 2010) reports that for ^{90}Y and ^{32}P the doses in the voxels near the glass microspheres show differences of less than 3% with respect to the doses of sources without the glass.

A simplified head of a typical gamma camera was also included in the simulation. It comprises a NaI(Tl) scintillator (width: 37 cm, length: 52 cm, thickness: 0.95 cm) and a lead collimator (square hole: 2 mm, septa thickness: 0.2 mm, length: 43 mm) placed at a distance of 3 cm from the abdomen of the phantom. The energy window covered 10% around the 81 keV for ^{166}Ho and from 0.1 to 2 MeV for ^{90}Y. For each event, the deposited energy and corresponding position (width and length coordinates) in the NaI(Tl) scintillator were recorded. The position and energy values were blurred using a Gaussian distribution with full width at half maximum of 4 mm and 10%, respectively, which are the typical resolutions of a gamma camera system for these quantities. The gamma camera images were generated with resolution of 256×256 pixels in gray scale proportional to the deposited energy. Fig. 1 shows a visualization of the objects included in the simulation: the NaI(Tl) scintillator, the collimator and only a section of the voxelized MASH phantom to make possible the visualization of internal organs and the tumor at the left lobe.

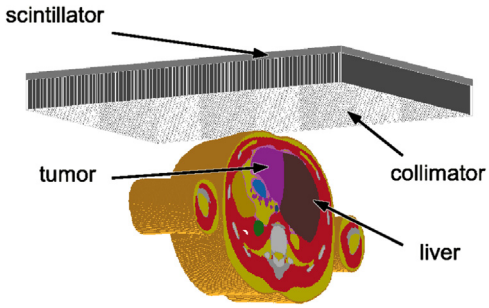

Fig. 1. Section of the voxelized MASH phantom and the detector of a gamma camera simulated with GEANT4. Tumor at the left lobe of the liver.

Simulations with ^{166}Ho and ^{90}Y were performed for cases of tumors with 15% of the liver mass localized in the seven possible positions mentioned above using 2×10^7 histories for each case. For each simulated history, one tumor voxel was randomly chosen and one radioactive nucleus was placed in its center. The output of the program produces three files: a text file with a list of the total dose per activity (Gy/GBq) for each organ, a binary file with the map of the dose per activity for each voxel, and a binary file in gray scale with the image of the gamma camera.

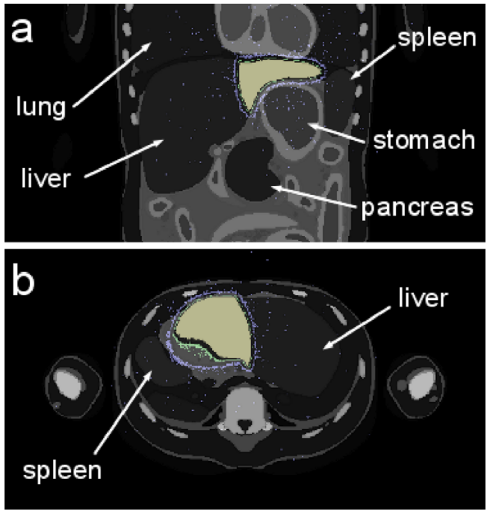

Fig. 2. Radiation source: ^{90}Y. Anteroposterior (a) and superior (b) views of slices of the voxelized MASH phantom superimposed by isodose voxels. Tumor at the left lobe of the liver with 15% of the liver volume. Yellow: 110–120 Gy; green: 30–45 Gy; blue: 0.2–2 Gy. (For interpretation of the references to color in this figure caption, the reader is referred to the web version of this article.)

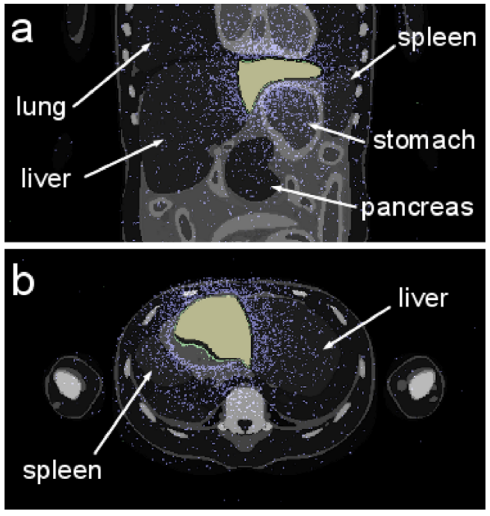

Fig. 3. Radiation source: ^{166}Ho. Anteroposterior (a) and superior (b) views of slices of the voxelized MASH phantom superimposed by isodose voxels. Tumor at the left lobe of the liver with 15% of the liver volume. Yellow: 110–120 Gy; green: 30–45 Gy; blue: 0.2–2 Gy. (For interpretation of the references to color in this figure caption, the reader is referred to the web version of this article.)

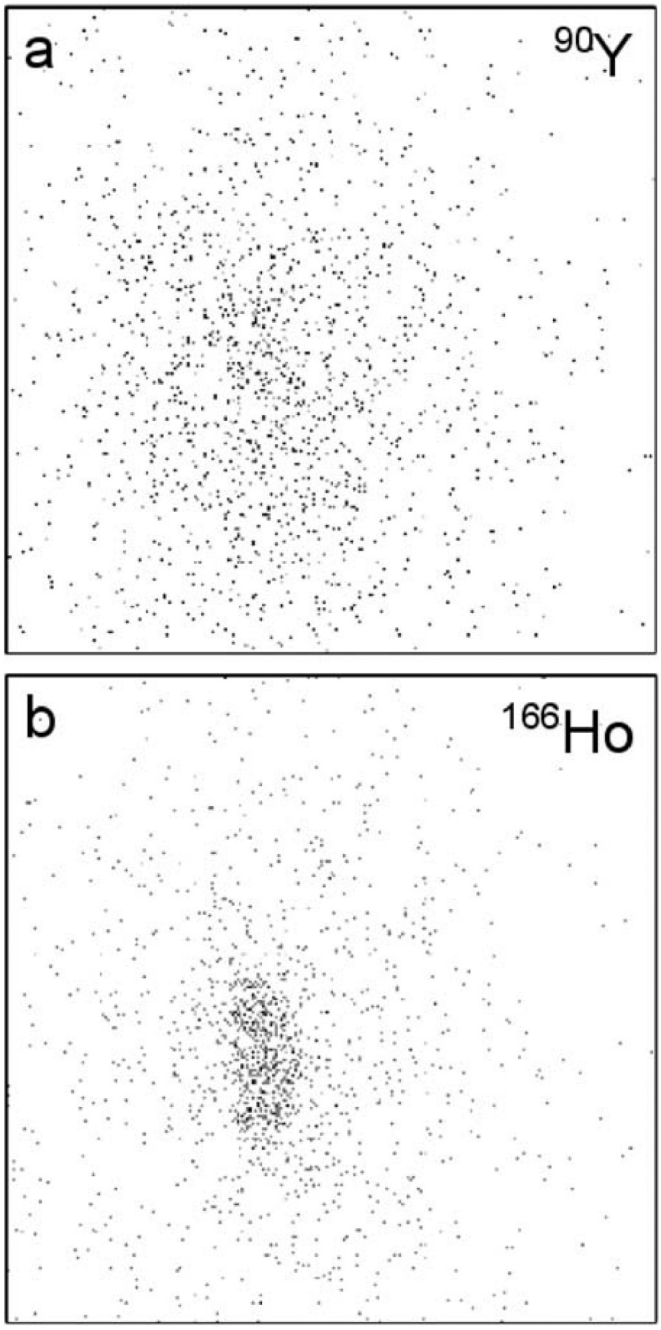

Fig. 4. Planar images of the gamma camera for a tumor with 15% of the liver volume at the lower extremity of the liver with ^{90}Y source (a) and ^{166}Ho source (b). Image resolution: 256 × 256 pixels.

3. Results

Figs. 2 and 3 show slices of the voxelized MASH phantom superimposed by isodose voxels calculated with GEANT4 for ^{90}Y and ^{166}Ho sources, respectively. As expected for this type of treatment, most of the dose is concentrated in the voxels of tumor and adjacent organs. On the two different slices one notices that the isodose voxels for the more energetic electrons of ^{90}Y reach few millimeters farther from the tumor than in the case of ^{166}Ho. The effect of the 81 keV gamma rays of ^{166}Ho is also noticed by the presence of doses from 0.2 to 2 Gy in the voxels surrounding the liver through the whole phantom section.

The results for different tumor positions show that, besides the healthy liver tissue, several organs are inside the range of the beta particles that leave the tumor. Although no other whole organ received a dose that could lead to failure, parts of some organs that are adjacent to the tumor can receive doses that reach 60 Gy. This occurs, for example, in the stomach wall when the tumor is at the left lobe of the liver, and in the right kidney when the tumor is at the inferior part of the liver. Other organs whose parts receive similar doses are the gallbladder, peritoneum and lymphatic nodes.

Fig. 4 shows the planar gamma camera images for similar simulations with ^{166}Ho and ^{90}Y for a tumor with 15% of the liver volume. Although the images have low statistics, one can notice the difference between the tumor localization using the 81 keV of ^{166}Ho with respect to the bremsstrahlung radiation of ^{90}Y.

4. Conclusion and perspectives

The GEANT4 Monte Carlo toolkit and an anthropomorphic phantom were employed to simulate the irradiation effects of liver tumor treatments with glass microspheres loaded with ^{166}Ho and ^{90}Y. The dose map as well as the image supplied by a typical planar gamma camera, which is used to localize the radiation sources, were produced successfully. Comparison between the results for ^{166}Ho with respect to ^{90}Y confirms that the source localization of ^{166}Ho is more precise without loss of effectiveness in the treatment.

There is the perspective of building an application with GEANT4 for the treatment planning, based on anatomical information about the patient's tumor region obtained with conventional imaging methods (CT, MR, SPECT, PET). This would require some improvements in the code, as for instance, to take into account the possible shunt to lungs and non-uniform distribution of the microspheres. More accurate results can be also reached by including the effects of the glass matrix where the radioactive sources are embedded.

Acknowledgments

This work has been supported by Centro de Radiofarmácia – IPEN.

References

Agostinelli, S., Allison, J., Amako, K., et al., 2003. GEANT4—a simulation toolkit. Nucl. Instrum. Methods Phys. Res., Sect. A 506, 250–303.

Barros Filho, E.C., Martinelli, J.R., Sene, F.F., 2012. Study of the spheronization process of glass particles for internal selective radiotherapy application. Mater. Sci. Forum 727-728, 1205–1210.

Cassola, V.F., de Melo Lima, V.J., Kramer, R., Khoury, H.J., 2010. FASH and MASH: female and male adult human phantoms based on polygon mesh surfaces. I. Development of the anatomy. Phys. Med. Biol. 55, 133–162.

Guimarães, C.C., Moralles, M., Sene, F.F., Martinelli, J.R., 2010. Dose-rate distribution of brachytherapy ^{32}P-glass microspheres for intra-arterial brachytherapy. Med. Phys. 37, 532–539.

Kramer, R., Khoury, H.J., Vieira, J.W., Lima, V.J.M., 2006. MAX06 and FAX06: update of two adult human phantoms for radiation protection dosimetry. Phys. Med. Biol. 51, 3331–3346.

Nijsen, J.F.W., Zonnenberg, B.A., Woittiez, J.R.W., Rook, D.W., Swildens-vanm Woudenberg, I.A., van Rijk, P.P., van het Schip, A.D., 1999. Holmium-166 poly lactic acid microspheres applicable for intra-arterial radionuclide therapy of hepatic malignancies: effects of preparation and neutron activation techniques. Eur. J. Nucl. Med. 26, 699–704.